

# Nature of the two quantum critical points in $\text{Ce}(\text{Ru}_{1-x}\text{Rh}_x)_2\text{Si}_2$ ( $x=0.4$ and $0.6$ )

J. S. Kim, D. J. Mixson, D. Burnette, B. Andraka, K. Ingersent, and G. R. Stewart  
*Department of Physics, University of Florida, Gainesville, Florida 32611-8440, USA*

E. W. Scheidt and W. Scherer

*Fachbereich Physik, Universitaet Augsburg, 86159 Augsburg, Germany*

(Received 28 April 2006; revised manuscript received 21 August 2006; published 20 October 2006)

The magnetic phase diagram of  $\text{Ce}(\text{Ru}_{1-x}\text{Rh}_x)_2\text{Si}_2$  contains a spin-density-wave (SDW) magnetic ordering temperature approaching  $T=0$  at both  $x \approx 0.03$  and  $0.35-0.4$  (i.e., a dome-shaped phase boundary) and long range, local moment antiferromagnetism,  $T_N=36$  K, in pure  $\text{CeRh}_2\text{Si}_2$  suppressed with Ru doping to  $T=0$  at  $x \approx 0.6-0.65$ . This latter possible second quantum critical point (QCP), and the possible interplay between the fluctuations caused at each of the two QCP's, are investigated here using specific heat, resistivity, and dc-magnetic susceptibility data over a broad range of composition, from  $x=0.04$  to  $0.8$ . One principal result is that the specific heat divided by temperature,  $C/T$ , for  $x=0.6$  ( $0.65$ ) near  $T_{\text{local moment}} \rightarrow 0$  is proportional to  $\log T$  over  $2\ 1/2$  decades of temperature down to the lowest temperature of measurement,  $0.04$  ( $0.3$ ) K, indicative of strong fluctuations near a QCP. For the region in the phase diagram  $x=0.4-0.5$ , i.e., near the reported  $T_{\text{SDW}} \rightarrow 0$  composition,  $C/T$  measured down to  $0.08$  K in the present work, as well as literature data, show a distinctly different behavior with temperature, a saturation in  $C/T$  which can be fit by  $\gamma - a\sqrt{T}$ . Such a temperature dependence is consistent with a nearby QCP with weakly interacting spin fluctuations as proposed, e.g., in the theory of Moriya. In the region between the two QCP's, at  $x=0.55$ , specific heat data down to  $0.1$  K are not well fit by  $C/T = \gamma - a\sqrt{T}$  and are consistent with  $C/T \sim \log T$  only down to  $0.6$  K, i.e., this composition displays intermediate behavior. The residual resistivity,  $\rho_0$ , vs  $x$  shows two strong peaks, at  $x=0.4$  and  $0.65$ , consistent with the existence of two quantum critical points. The exponent  $\alpha$  in  $\rho = \rho_0 + AT^\alpha$  indicates non-Fermi liquid behavior, with  $\alpha$  varying monotonically—in contrast to  $\rho_0$ —from  $1.5$  to  $\sim 0.9$  between  $x=0.3$  and  $0.65$ . The Fermi liquid exponent,  $\alpha=2$ , is recovered at  $x=0.8$ . These results taken together indicate two *distinct* quantum critical points in the phase diagram of  $\text{Ce}(\text{Ru}_{1-x}\text{Rh}_x)_2\text{Si}_2$ , with different fluctuation strengths at  $x$  ( $T_{\text{SDW}} \rightarrow 0$ )  $= 0.4$  and  $x$  ( $T_{\text{local moment}} \rightarrow 0$ )  $\approx 0.6-0.65$ .

DOI: [10.1103/PhysRevB.74.165112](https://doi.org/10.1103/PhysRevB.74.165112)

PACS number(s): 71.10.Hf, 71.27.+a, 75.20.Hr

## I. INTRODUCTION

Characterization of the pseudoternary phase diagram between  $\text{CeRu}_2\text{Si}_2$  and  $\text{CeRh}_2\text{Si}_2$  has been a subject of interest<sup>1-20</sup> for the last two decades, i.e., starting even before the experimental discovery<sup>21</sup> of non-Fermi liquid (nFL) behavior in  $\text{U}_{0.2}\text{Y}_{0.8}\text{Pd}_3$ . In addition, there has been characterization of the endpoint system properties:  $\text{CeRu}_2\text{Si}_2$  as a heavy Fermion system<sup>22</sup> with interesting behavior<sup>23,24</sup> at its 8 T metamagnetic phase transition and  $\text{CeRh}_2\text{Si}_2$  for its intriguing magnetic behavior<sup>8,25</sup> and its pressure induced superconductivity.<sup>26</sup> Since the discovery<sup>21</sup> of nFL behavior<sup>27</sup> in  $\text{U}_{0.2}\text{Y}_{0.8}\text{Pd}_3$ , discussion has tended to focus on non-Fermi liquid behavior/quantum critical behavior at concentrations  $x \leq 0.5$  in the  $\text{Ce}(\text{Ru}_{1-x}\text{Rh}_x)_2\text{Si}_2$  phase diagram. The previous work on  $\text{Ce}(\text{Ru}_{1-x}\text{Rh}_x)_2\text{Si}_2$  has used various measurement techniques at the different concentrations:  $x=0.03$  (Refs. 14 and 19)/specific heat, neutron scattering;  $x=0.07-0.2$  (Refs. 4 and 14)/specific heat, magnetic susceptibility;  $x=0.3$  (Refs. 1-3 and 14)/specific heat, magnetic susceptibility;  $x=0.35$  (Refs. 4 and 7)/specific heat, resistivity;  $x=0.4$  (Refs. 1, 3, 15, and 18)/specific heat, magnetic susceptibility, resistivity;  $x=0.5$  (Refs. 1, 5, 6, 10-13, 16-18, and 20)/specific heat, magnetic susceptibility, resistivity,  $\mu\text{SR}$ ;  $x=0.55$  (Ref. 5)/specific heat;  $x=0.6$  (Refs. 2, 5, 10, and 13)/specific heat, magnetic susceptibility. As will be discussed more thoroughly below when the results of the present work are com-

pared to the extant literature, these cited measurements were sometimes in conflict with each other for  $x=0.4$  and  $0.5$ .

What would be the behavior *between* two quantum critical points? One of the candidate systems to investigate this is indeed  $\text{Ce}(\text{Ru}_{1-x}\text{Rh}_x)_2\text{Si}_2$ . The phase diagram of this system contains a spin density wave (SDW) transition, reported<sup>1,7,9,13,14</sup> to go to  $T=0$  at  $x \approx 0.35-0.4$  and a local moment antiferromagnetic transition starting at the  $\text{CeRh}_2\text{Si}_2$  side of the phase diagram at  $T_N=36$  K, variously reported<sup>1,2,9,13</sup> to be suppressed to  $T=0$  at  $x \approx 0.5-0.6$ . In order to investigate the behavior between two QCP's and to resolve the position of, and better characterize, the local moment QCP, the present work—using measurements of the specific heat down to  $0.04$  K and the resistivity to  $0.3$  K to determine the presence or absence of non-Fermi liquid behavior—was carried out. Samples were characterized both on the Ru-rich side of the phase diagram in the vicinity of where  $T_{\text{SDW}} \rightarrow 0$  ( $x=0.3, 0.4, 0.45, 0.5$ ) and on the Rh-rich side of the phase diagram ( $x=0.55, 0.6, 0.65, 0.7$ , and  $0.8$ .) As discussed above, numerous works<sup>1-7,10-18,20</sup> have studied  $0.3 \leq x \leq 0.5$  in  $\text{Ce}(\text{Ru}_{1-x}\text{Rh}_x)_2\text{Si}_2$ . In contrast, noticeably fewer works<sup>2,5,10,13</sup> have studied  $x=0.55$  and  $0.6$ —of which the first two<sup>2,5</sup> were from before the pioneering work<sup>21</sup> on  $\text{U}_{0.2}\text{Y}_{0.8}\text{Pd}_3$  and were not analyzed for possible non-Fermi liquid behavior, while the later work<sup>10,13</sup> reported low field ac susceptibility but not specific heat or resistivity.

In addition, a sample with  $x=0.04$  was measured in order to provide additional specific heat data as input to the

TABLE I. X-ray, resistivity, and magnetic susceptibility results for polycrystalline  $\text{Ce}(\text{Ru}_{1-x}\text{Rh}_x)_2\text{Si}_2$ . The last column quantifies the size of the magnetic anomaly at  $\sim 13$  K for  $x \geq 0.6$ . The value of  $\chi(2$  K) reported here for  $x=0.5$  is consistent with the (weighted) average of the  $c$ -axis and  $a$ -axis single crystal values reported in the literature (Ref. 1). Since there is a strong anomaly in  $C$  and  $\chi$  for  $x=0.8$  at approximately the same ordering temperature as for  $x=0.9$ , and since (Ref. 29) the smearing of the high angle x-ray lines for  $x=0.8$  is larger than for lower concentrations, there is presumably phase separation at  $x=0.8$ . This does not appear to affect the trend observed in  $\rho_0$ , see data below and plotted in Fig. 2.

$x$	$a$ -/ $c$ -axis (Å)	$\rho_0$ ( $\mu\Omega$ cm)	RRR [ $\rho(300$ K)/ $\rho_0$ ]	$\alpha$ ( $\rho=\rho_0+AT^\alpha$ )	$\chi(2$ K) (memu)	$\frac{\chi(2$ K)- $\chi(12$ K) $\chi(12$ K)
0.3	4.1756/9.8520	100	4.0	1.5	23	
0.4		185	3.4	1.3	90	
0.45	4.1546/9.9320	140	3.1	1.2	32	
0.5		125	3.4	1.2	27	
0.55		70	3.0	1.1	24.5	
0.6	4.1459/9.9709	80	2.7	0.9	23	0.2
0.65		130	2.8	0.9	18	$\sim 0$
0.8	4.1129/10.0894	60	3.3	2	7	-0.6

discussion<sup>19</sup> of the possibility of non-Fermi liquid near a QCP near the Rh-*poor* limit of the dome-shaped SDW phase boundary.

## II. EXPERIMENTAL

Resistivity,  $\rho$ , was measured down to 0.3 K using a 4-wire dc technique; magnetic susceptibility,  $\chi$ , was measured down to 2 K using a Quantum Design MPMS system. Specific heat,  $C$ , was measured using techniques discussed thoroughly previously.<sup>28</sup> Polycrystalline samples were prepared by arc melting together the pure constituents (including high purity Ce metal, 99.99% pure, from Ames and 99.9999% pure Si, 99.95% pure Ru, and 99.95% pure Rh from Alpha Aesar) under a purified argon atmosphere, followed by remelting twice to assure homogeneity. Mass losses were less than 0.2%.

X-ray diffraction results of these tetragonal compounds indicated no other structures were present. For  $\text{CeRu}_2\text{Si}_2$ , the lattice parameters determined were  $a=4.1964$  Å and  $c=9.7965$  Å while for  $\text{CeRh}_2\text{Si}_2$ ,  $a=4.0883$  Å and  $c=10.1813$  Å, i.e., the basal plane shrinks and the  $c$  axis expands as Rh is added to  $\text{CeRu}_2\text{Si}_2$ . Representative lattice parameters for the  $\text{Ce}(\text{Ru}_{1-x}\text{Rh}_x)_2\text{Si}_2$  samples,  $0.3 \leq x \leq 0.8$ , are given in Table I. A feature of the Rh-rich side of one<sup>2,9</sup> of the published magnetic phase diagrams is that the magnetic ordering temperature appears to “pin” at around 13 K all the way from  $x=0.9$  down to  $x=0.6$ , while another<sup>1</sup> phase diagram shows, albeit with a sparser data set, more monotonic suppression of  $T_N$  with Ru doping on the Rh-rich side. We have addressed this discrepancy and present data here<sup>29</sup> demonstrating that the pinned  $T_N$  is due to phase separation occurring for  $x < 0.9$ , with a significant anomaly at 13 K in the specific heat (with  $0.5R \ln 2$  of entropy) at  $x=0.8$  decreasing to a minor anomaly (with  $0.03R \ln 2$  of entropy) by  $x=0.6-0.65$ . This phase separation into Rh-richer and Rh-poorer regions causes, according to x-ray measurements, broadening of high angle line widths that is visible on both

sides of the phase diagram, at  $x \sim 0.2$  and 0.8. In the composition range studied in the present work ( $0.3 \leq x \leq 0.8$ ), the phase separation is apparent in magnetic measurements (with a lower temperature limit of 2 K) only on the Rh-rich, local moment side of the phase diagram. Our data are consistent with minor amounts of Rh-rich material (perhaps<sup>29</sup> due to spinodal composition upon cooling from the melt) for  $0.6 \leq x < 0.8$  that give an anomaly in  $\chi$  (Ref. 2, see also Fig. 1 below) at 13 K mimicking the behavior of the majority phase with a concentration more like  $x=0.9$ , for which composition the bulk or intrinsic  $T_N$  is 13 K. A phase diagram<sup>2</sup> not based on a bulk measure of the presence of magnetism can conclude that  $T_N$  remains constant over the concentration region where there is phase separation.

Fortunately for the present work, the amount of phase separation, quantifiable via the size of the specific heat anomaly at 13 K, decreases rapidly as  $x$  is decreased below 0.8 and is negligible for  $x \leq 0.65$  where our measurements indicate quantum critical behavior in the specific heat. For the majority of the discussion below, we focus on the intrinsic, majority phase behavior, with brief mentions of the  $\chi$  and  $C$  anomalies at 13 K due to phase separation.

## III. RESULTS AND DISCUSSION

### A. Susceptibility and resistivity

The low temperature magnetic susceptibility data for the samples of the present work, see Fig. 1 and Table I, show definite upturns in  $\chi$  vs  $T$  with decreasing temperature for  $x=0.55$  and 0.6, characteristic of non-Fermi liquid behavior, and a slight upturn for  $x=0.65$ . Due to the structure in the low temperature  $\chi$  data as displayed in Fig. 1 (data for  $x=0.45$ , not shown, are similar to those for  $x=0.55$ ), the temperature dependence of these data is obscured for purposes of comparing with the various possible theoretically predicted non-Fermi liquid behaviors.

These  $\chi$  data also allow the (nonbulk) determination of the depression of the long range antiferromagnetic order in

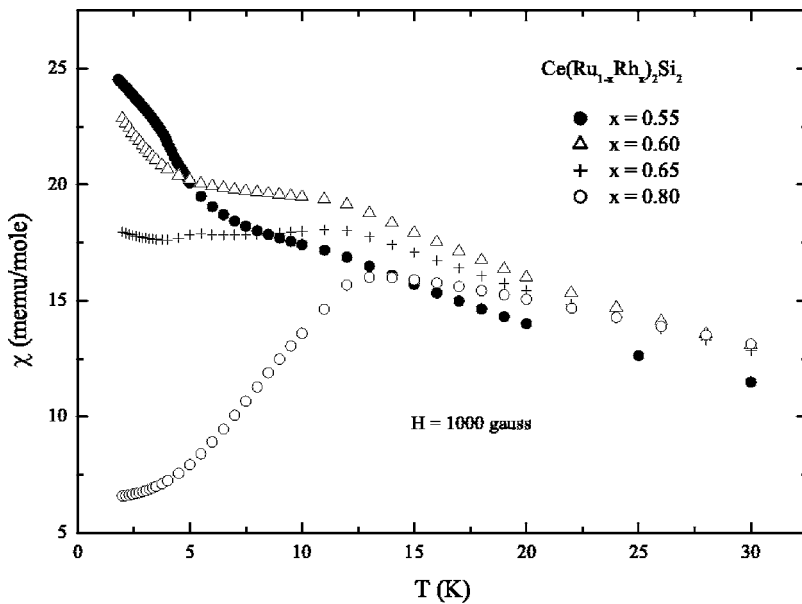


FIG. 1. Magnetic susceptibility of  $\text{Ce}(\text{Ru}_{1-x}\text{Rh}_x)_2\text{Si}_2$  around the local moment quantum critical point. Note the substantial anomaly for  $x=0.8$  which is much reduced in magnitude by  $x=0.60$ , although still at the same temperature. This remanent anomaly at 13 K in these  $\chi$  data is due to phase separation (Ref. 29); the upturns below 5 K in the data appear to be intrinsic and associated with the non-Fermi liquid behavior observed in the other properties.

pure  $\text{CeRh}_2\text{Si}_2$ ,  $T_N=36$  K, with increasing Ru content in  $\text{Ce}(\text{Ru}_{1-x}\text{Rh}_x)_2\text{Si}_2$ . Consistent with the magnetic phase diagram of Refs. 2 and 9, Table I and Fig. 1 show that the anomaly in  $\chi$  vs  $T$  is suppressed to  $\sim 13$  K by  $x=0.8$ , see also Fig. 2. As will be seen from the specific heat discussed below, the lessening of the size of the anomaly at 13 K in  $\chi$  vs  $T$  with increasing Ru doping (see Fig. 1 and the right hand column of Table I) corresponds to a factor of 15 lessening of the entropy  $[S=\int(C/T)dT]$  associated with the magnetic ordering from  $x=0.8$  to  $x=0.65$  and 0.6. Based on the line

broadening observed in the x-ray data discussed above, the slight remanent indications of magnetism at 13 K seen in the  $\chi$  data, Fig. 1, for  $x=0.65$  and 0.6 are presumably due<sup>29</sup> to a small amount of phase separation.

Although the dc-magnetic susceptibilities shown in Fig. 1 for  $x=0.55$  and 0.6 show definite divergent (non-Fermi liquid) behavior only between 2 (the lowest temperature of measurement in the present work) and approximately 5 K, there are literature results for  $x=0.6$  (Refs. 10 and 13) for ac-magnetic susceptibility as well as both dc- and ac-

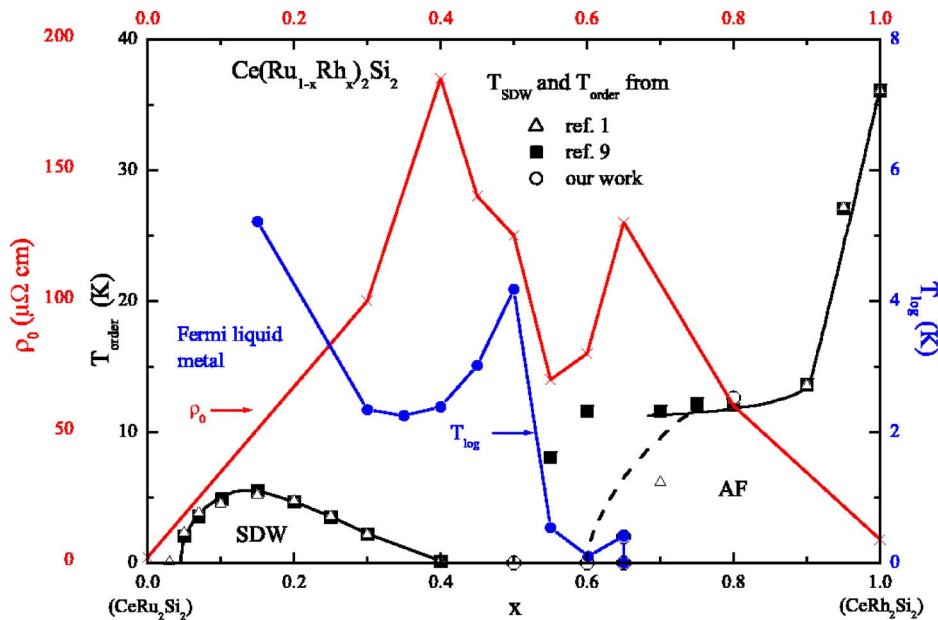


FIG. 2. (Color online) Two possible magnetic phase diagrams from the literature (Refs. 1 and 9) vs  $x$  for  $\text{Ce}(\text{Ru}_{1-x}\text{Rh}_x)_2\text{Si}_2$ , displaying the possibility present for two quantum critical points at  $x=0.4$  ( $T_{\text{SDW}} \rightarrow 0$ ) and  $x \sim 0.6-0.65$  ( $T_{\text{local moment}} \rightarrow 0$ ). The present work finds (Ref. 29) that the “pinning” of  $T_{\text{local moment}}$  at  $\sim 13$  K between  $x=0.6$  and 0.8 is due to phase separation. Specific heat data, discussed below in Fig. 5, find no appreciable bulk fraction of the sample undergoes magnetic order for  $x \leq 0.65$ .  $T_{\text{log}}$ , the temperature down to which  $C/T \sim \log T$  is plotted as the solid circles (●) against the right vertical axis, while  $\rho_0$  as a function of  $x$ , using data from Table I, is plotted against the left most vertical axis. Lines connecting the points are guides to the eye. For  $x=0.65$ , since  $T_{\text{log}}$  may extend below 0.3 K, our lowest temperature of measurement for this composition, the value for  $T_{\text{log}}$  is represented as two points connected by a line.

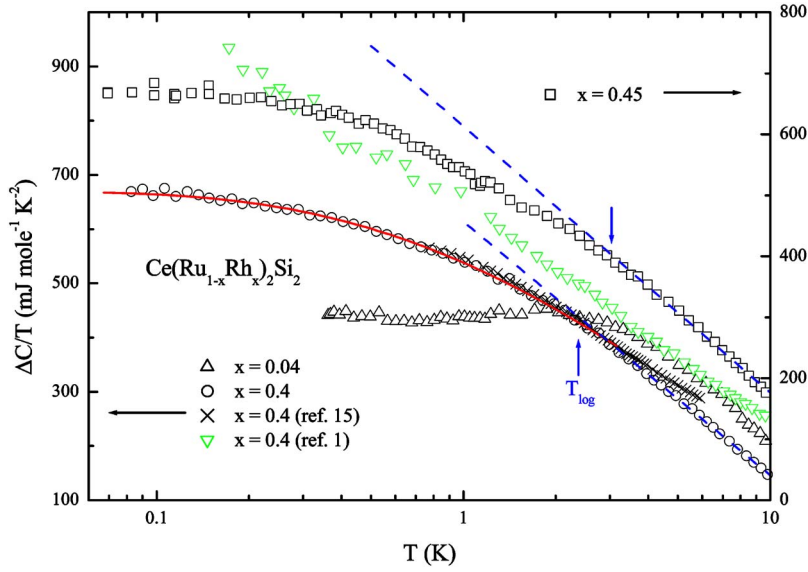


FIG. 3. (Color online) Electronic specific  $\Delta C$  (corrected for the lattice contribution via subtraction of the lattice specific heat of  $\text{LaRu}_2\text{Si}_2$ ) divided by temperature,  $T$ , of  $\text{Ce}(\text{Ru}_{1-x}\text{Rh}_x)_2\text{Si}_2$  for  $x=0.04$ ,  $0.4$ , and  $0.45$  as discussed in the text. The solid line (—) is a fit of the data from the present work for  $x=0.4$  to the weak spin fluctuation theory of Moriya (Ref. 37). The dashed lines (---) show the  $\log T$  behavior of the higher temperature data for  $x=0.4$  and  $0.45$  down to  $T_{\log}$ .

susceptibility for  $x=0.5$  (Refs. 10, 13, and 20) to temperatures as low as 0.04 K. These data have been analyzed<sup>10,13,20</sup> in terms of disorder models for nFI behavior (the Kondo disorder model and the Griffiths phase spin cluster model). In addition, NMR and  $\mu\text{SR}$  measurements<sup>16</sup> on  $\text{Ce}(\text{Ru}_{1-x}\text{Rh}_x)_2\text{Si}_2$ ,  $x=0.5$ , have been used to further understand these<sup>10,13,20</sup> data. These results will be discussed with the specific heat results for  $x=0.5$  and  $0.6$  below.

The resistivities between 0.3 and 1.5 K of the polycrystalline samples of the present work follow  $\rho = \rho_0 + AT^\alpha$ , with  $\alpha$  approximately temperature independent. As shown in Table I,  $\alpha$  decreases from 1.5 (the exponent expected<sup>27</sup> by various theories for weak antiferromagnetic fluctuations in a three-dimensional system) at  $x=0.3$  to a number slightly less than 1 for  $x=0.6$  and  $0.65$ . Non-Fermi liquid systems often<sup>27</sup> display  $\alpha \approx 1$ . The exponent expected for Fermi liquid behavior,  $\alpha=2$ , is found<sup>23</sup> in pure  $\text{CeRu}_2\text{Si}_2$ , and is recovered with increasing Rh doping by  $x=0.8$ , see Table I.

The residual resistivity values shown in Table I for polycrystalline  $\text{Ce}(\text{Ru}_{1-x}\text{Rh}_x)_2\text{Si}_2$  are large compared to the  $\rho_0 = 2 \mu\Omega \text{ cm}$  for pure<sup>23</sup>  $\text{CeRu}_2\text{Si}_2$ , as is typical of doped highly correlated electron systems, e.g., 5% Pd doping on the Pt site in  $\text{UPt}_3$  increases<sup>30</sup>  $\rho_0$  from 6 to  $100 \mu\Omega \text{ cm}$ . It is interesting to note the two pronounced maxima in  $\rho_0$  as a function of  $x$  at  $x=0.4$  and  $0.65$  (not at  $x=0.5$  as expected by Nordheim's rule) shown in Table I and graphically in Fig. 2. A maximum in  $\rho_0$  can indicate where a QCP is in a phase diagram, e.g., in  $\text{Sr}_3\text{Ru}_2\text{O}_7$  as a function of field<sup>31</sup> or in  $\text{CeNi}_{1-x}\text{Co}_x\text{Ge}_2$  as a function of doping.<sup>32</sup> Although some contribution to  $\rho_0$  can be expected in  $\text{Ce}(\text{Ru}_{1-x}\text{Rh}_x)_2\text{Si}_2$  from the phase separation, this contribution should be largest where<sup>29</sup> the phase separation is largest, at  $x \sim 0.8$  and  $0.2$ , and Table I and Fig. 2 show that  $\rho_0$  shows no hint of maxima or structure at these compositions. Furthermore, in, e.g., the strongly correlated system  $\text{U}_{1-x}\text{M}_x\text{Al}_2$ ,  $M=\text{Lu}, \text{Ce}, \text{La}, \text{Y}, \text{Sc}, \text{and Zr}$ , which shows strong phase separation,  $\rho_0$  shows<sup>33</sup> essentially no structure due to the phase separation but rather the typical Nordheim-type broad maximum at  $x=0.5$  ( $\rho_0^{\text{max}} \sim 100 \mu\Omega \text{ cm}$ ), with  $\rho_0 = 5 \mu\Omega \text{ cm}$  for pure  $\text{UAl}_2$ .

A second comparison of the  $\rho_0$  values for polycrystalline  $\text{Ce}(\text{Ru}_{1-x}\text{Rh}_x)_2\text{Si}_2$  shown in Table I and Fig. 2 is with values

obtained for single crystals. Literature data for single crystal resistivity data for  $\text{Ce}(\text{Ru}_{1-x}\text{Rh}_x)_2\text{Si}_2$  are:  $\rho_0 = 64(17) \mu\Omega \text{ cm}$  for current in the  $a$ -axis<sup>20</sup> ( $c$ -axis<sup>11</sup>) direction for  $x=0.5$  [no residual resistivity ratio (RRR) values given<sup>11,20</sup>] and  $\rho_0 = 40 \mu\Omega \text{ cm}$  (RRR  $\sim 2.75$ ) for<sup>34</sup> current in the  $a$ -axis direction for  $x=0.8$ . Thus, although disorder in the polycrystalline sample compared to the single crystal for  $x=0.8$  is evident in the larger  $\rho_0$  value for the former ( $\rho_0 = 60 \mu\Omega \text{ cm}$  and RRR=3.3 for polycrystalline  $x=0.8$ , Table I) the RRR values are fairly comparable. The issue of whether the disorder inherent with doping Rh on the Ru site affects the bulk specific heat properties will be discussed below.

## B. Specific heat and non-Fermi liquid behavior

$x=0.04$ : We begin the discussion with the left side of the magnetic phase diagram shown in Fig. 2, starting with small Rh doping of  $\text{CeRu}_2\text{Si}_2$ . The low temperature specific heat divided by temperature,  $C/T$ , of  $\text{Ce}(\text{Ru}_{0.96}\text{Rh}_{0.04})_2\text{Si}_2$  (see Fig. 3) is essentially constant (Fermi liquid behavior) between 0.3 and 2 K, with a low temperature intercept,  $\gamma$ , of  $430 \text{ mJ/mol K}^2$ —approximately 15% higher than the  $385 \text{ mJ/mol K}^2$  measured for pure  $\text{CeRu}_2\text{Si}_2$  (by others<sup>22</sup> and also in our own laboratory<sup>35</sup>).  $C/T$  data in the literature for  $x=0.03$  (Refs. 14 and 36) and  $0.05$  (Ref. 36) vary significantly in magnitude at low temperatures but agree with the finding of the present work for  $x=0.04$  that  $C/T$  is essentially constant at low temperatures. Despite the interesting enhancement in  $\gamma$  observed in the present work near the Rh-poor  $T_{\text{SDW}} \rightarrow 0$  phase boundary, this saturated, constant  $C/T$  behavior as  $T \rightarrow 0$  is not indicative of non-Fermi liquid behavior due to a quantum critical point nearby in the phase diagram. This is in contrast to the recent<sup>19</sup> non-Fermi liquid exponent found in the dynamical susceptibility behavior at 1.5 K as measured by neutron scattering for an  $x=0.03$  sample.

$x=0.3$ : The specific heat data of the present work (not shown) down to 0.3 K for  $\text{Ce}(\text{Ru}_{0.7}\text{Rh}_{0.3})_2\text{Si}_2$  agree within a few percent with published data<sup>1,3,14</sup> and show  $C/T \sim \log T$

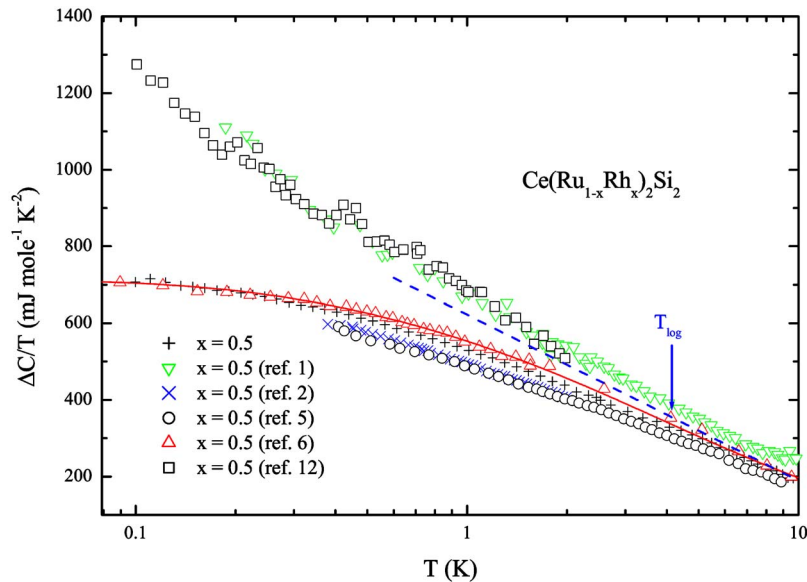


FIG. 4. (Color online) Electronic specific  $\Delta C/T$  of  $\text{Ce}(\text{Ru}_{1-x}\text{Rh}_x)_2\text{Si}_2$  for  $x=0.5$ . Solid line (—) is a fit of the data from Ref. 6 to the weak spin fluctuation theory of Moriya (Ref. 37). The dashed line (- -) shows that these data do not obey  $C/T \sim \log T$  below  $\sim 4$  K.

from 10 K down to about 2.5 K and  $C/T \rightarrow \text{const.}$  below about 1.5 K. This Fermi liquid behavior at low temperatures in the specific heat is in contrast to the  $\rho = \rho_0 + AT^{1.5}$  non-Fermi liquid behavior observed in the resistivity, Table I. Since resistivity often<sup>27</sup> shows Fermi liquid behavior beginning at a *lower* temperature than other measurement techniques, measurements to below 0.3 K may show  $\alpha \rightarrow 2$ .

$x=0.4$ : In addition to data for  $x=0.04$ , Fig. 3 also shows  $C/T$  data for  $x=0.4$  from the literature<sup>15</sup> for a Czochralski-method single crystal together with the data on polycrystalline material taken in the present work. Both sets of data agree fairly well in their temperature region of overlap—the data of Ref. 15 were measured only down to 0.8 K in a Be-Cu piston in measurements under pressures from zero up to 1.6 GPa—and show a tendency towards saturation at low temperature. However, data<sup>1,3</sup> on a Czochralski-method single crystal measured by another group (Refs. 1 and 3 contain the same set of data) disagree with these data as shown in Fig. 3, and show approximately  $C/T \sim \log T$  (i.e., divergent, not saturation behavior) down to 0.15 K, as well as a significant disagreement (22% at 0.4 K) in the magnitude of the data. However, if the eight data points, which show some scatter, in Refs. 1 and 3 below 0.35 K are discarded, the data indicate rather saturation in  $C/T$ , agreeing with the temperature dependence of the present work's data set of 18 low-scatter points below 0.35 K with, however, still a disagreement in the magnitude of the  $C/T$  data. The same type of discrepancy also exists for  $x=0.5$  and will therefore be further discussed below.

Focusing now on the two data sets that are in agreement for  $x=0.4$  in Fig. 3, just as for the  $x=0.3$  data discussed above,  $C/T \sim \log T$  from 10 K down to about 2.5 K for the data from the present work and that from Ref. 15, at which point the data tend towards saturation. Our data for  $x=0.4$  between 0.08 and 2.5 K can be fit to the Moriya theory<sup>37</sup> of weakly coupled spin fluctuations (solid line in Fig. 3). This fit gives  $y_0 = 0.004 \pm 0.002$ , where  $y_0$  in this theory approaches zero at the QCP, i.e., these data are at least consistent—within the Moriya model—with there being a

weak coupling QCP somewhere near  $x=0.4$ . The result of this fit is roughly consistent with the exponent of the temperature dependence measured in the resistivity for this composition of 1.3, since the Moriya theory would predict  $\alpha = 1.5$ . However, the Moriya theory fit to  $C/T$  has three adjustable parameters and is certainly not unique. Another possible fit would be the Kondo disorder model,<sup>27</sup> especially considering the unavoidable disorder introduced by substituting Rh for Ru in  $\text{Ce}(\text{Ru}_{1-x}\text{Rh}_x)_2\text{Si}_2$ . However, the Griffiths phase scenario<sup>27,38</sup> to explain disorder-induced nFl behavior—which predicts a power law behavior for  $C/T \sim T^{1+\lambda}$ —does *not* fit the  $x=0.4$  data shown in Fig. 3, since a log-log plot of the data (not shown) shows curvature over the whole temperature range.

$x=0.45$ :  $C/T$  data from the present work for  $x=0.45$  down to 0.1 K are also shown in Fig. 3. Here the  $C/T$  can be fit from 10 K only down to 3 K by  $\log T$ . These  $x=0.45$  data can be fit (not shown in Fig. 3) between 2 and 0.07 (lowest temperature of measurement) K to the Moriya theory where  $y_0 \rightarrow 0$  at the QCP, giving  $y_0 = 0.005 \pm 0.002$ . This is consistent with  $x=0.45$  not being *at* the quantum critical point in the Moriya theory but, within our error bar, is—just like for  $x=0.4$ —quite close to a QCP. The agreement in magnitude (note different y axis in Fig. 3) and temperature dependence between the data from the neighboring composition of  $x=0.45$  is consistent with the present work's results for  $x=0.4$ .

$x=0.5$ : As shown in Fig. 4, for  $x=0.5$  there is again good agreement between literature data<sup>2,5,6</sup> and the data of the present work, all for *polycrystalline* samples. Figure 4 shows that the published  $C/T$  data for  $x=0.5$  from Refs. 2 and 5 measured down to  $\sim 0.3$  K and  $C/T$  data from Ref. 6, measured down to 0.08 K, agree internally among the three sets of data (to within 8% at 0.3 K) as well as with the data of the present work, with  $C/T(0.3 \text{ K}) \sim 630 \text{ mJ/mol K}^2$ . However, just as for  $x=0.4$ , the same group's data<sup>1,12</sup> for  $x=0.5$ —measured again on Czochralski-method single crystals—disagree both in temperature dependence and magnitude below 2 K with the other literature data<sup>2,5,6</sup> and the

data of the present work—all in this case on polycrystalline material. Reference 1 notes this disagreement with the  $x=0.5$  data of Ref. 6 and ascribes the difference as possibly due to the difference in sample preparation, single vs polycrystalline material. This explanation still leaves open the discrepancy discussed above and shown in Fig. 3 for  $x=0.4$  where the data of Ref. 15 (which agree with the data of the present work) taken in a pressure clamp cell, with no pressure applied, are on a Czochralski-method single crystal just as the data of Ref. 1. This discrepancy can best be resolved with a study<sup>39</sup> of the properties of single crystal samples over a range of compositions.

Focusing now on the polycrystalline  $C/T$  data for  $x=0.5$ , the data can be fit to  $\log T$  only between 10 and just above 4 K as shown in Fig. 4. A fit of the present work's data for  $x=0.5$  to the Moriya theory (not shown) gives a value of  $y_0=0.001$ , or again very close to a QCP. We have also performed a fit (shown in Fig. 4) of the data down to 0.08 K from Ref. 6 to the theory of Moriya,<sup>37</sup> which gives  $y_0=0.004\pm 0.002$ , i.e., consistent with the fit to the data of the present work considering the error bar in the Moriya fitting procedure of  $\pm 0.002$ . The (within the error bars) equal values of  $y_0$  for  $x=0.4, 0.45$ , and  $0.5$  fail to indicate the usual<sup>27</sup> measurable trend in  $y_0$  as a function of doping that would indicate a QCP at  $T_{\text{SDW}} \rightarrow 0$  at some one particular concentration  $x$ , e.g.,  $x=0.4$ , in  $\text{Ce}(\text{Ru}_{1-x}\text{Rh}_x)_2\text{Si}_2$ . They are consistent, however, with the view that there is a weak coupling QCP somewhere in the vicinity of  $x=0.4-0.5$ , which is further consistent with the peak in  $\rho_0$  at  $x=0.4$  discussed above and shown in Fig. 2. It is interesting to note that the behavior of  $\rho_0$  vs  $x$  shows quite a sharp behavior, while the  $y_0$  values derived from the specific heat via the Moriya theory fits shows behavior apparently smeared out, possibly due to disorder affecting the specific heat.

However, the fit of the data to the Moriya model is not unique; in the original Ref. 6, the  $C/T$  data were fit to the Kondo disorder model, discussed in Ref. 27. The other usual candidate to describe nFI behavior in a disordered system, the Griffiths phase model,<sup>38</sup> can however *not* be used to fit the data for  $x=0.5$  in Fig. 4. When the  $C/T$  data are plotted (not shown) on a log-log plot to determine if they obey the Griffiths power law behavior,  $C/T \sim T^{1+\lambda}$ , there is no significant temperature region of linear behavior. This inability of the Griffiths phase model to fit the specific heat data in Fig. 4 contrasts with the interpretation of the published low temperature  $\chi$  data<sup>10,13,20</sup> for  $x=0.5$ . These low field,  $H \leq 100$  G, data (higher fields suppress the upturn in  $\chi$ ) diverge below 1 K as a Griffiths phase power law. NMR and  $\mu$  SR measurements<sup>16</sup> on  $x=0.5$  were found however to be inconsistent with both the Griffiths phase and the disordered Kondo models being the source of the nFI behavior at low temperatures.

Besides tracking the fit parameter  $y_0$  in the Moriya theory, another way to quantify the progression of the non-Fermi liquid behavior is to plot  $T_{\log}$ , defined as the lowest temperature where  $C/T$  can be fit to  $\log T$ . These  $T_{\log}$  values, mentioned above for the  $x=0.3, 0.4, 0.45$ , and  $0.5$  data as they were discussed and/or presented in the figures and for  $x=0.15$  and  $0.35$  from<sup>4</sup> the literature, are also shown in Fig. 2

plotted against the right hand vertical axis. There is a definite minimum in  $T_{\log}$  around the putative QCP at  $x=0.4$ .

$x=0.6$ : How do the non-Fermi liquid behavior and  $T_{\log}$  develop with increasing Rh doping, as the local moment antiferromagnetic order part of the phase diagram is approached? The only  $C/T$  data for  $x=0.6$  material extant in the literature are from Refs. 2 and 5 which both predate the discovery of nFI behavior in 1991, on polycrystalline samples. These data<sup>2,5</sup> for  $x=0.6$ , measured between 2 and 0.4 K and 8 and 0.3 K respectively, were scanned and are shown in Fig. 5. The  $C/T$  data are fit by  $\log T$  and show no signs of saturation or Moriya behavior. Clearly, data to lower temperatures would be useful in making a full determination. Data on a sample prepared for the present work were therefore measured down to the rather low temperature of 0.04 K. As may be seen in Fig. 5 these data (all on polycrystalline material) are well fit by  $C/T \sim \log T$  over a very large temperature range of measurement (2 1/2 decades) and a characteristic temperature  $T_0$  ( $C/T$  can be expressed<sup>27</sup> as  $R[0.25/T_0] \ln T$ ) of 23 K. There is perhaps some slight tendency to saturate below 0.07 K. This  $\log T$  behavior for polycrystalline  $x=0.6$  is in strong contrast to the saturation behavior for the  $C/T$  data for polycrystalline  $x=0.5$  shown in Fig. 4. This rapid change with composition in the temperature dependence of  $C/T$  is one of the interesting results from the present work. This quick change from  $C/T \rightarrow \text{const.}$  to  $C/T \sim \log T$  does not appear to be driven by disorder, since the difference in disorder between  $x=0.5$  and  $0.6$  should be *a priori* (see also the trend in  $\rho_0$  in Table I) the *same* as that between  $x=0.5$  and  $0.4$ , which both show the same temperature dependence in  $C/T$ .

Low temperature, low field ( $H \leq 100$  G)  $\chi$  data<sup>13</sup> for  $x=0.6$  have been interpreted using the Griffiths phase model to indicate the present of a quantum critical point at  $x=0.6$ . Fields above 100 G suppress the divergence below 1 K in  $\chi$ . Clearly the power law Griffiths model behavior cannot *a priori* fit the  $\log T$  dependence for  $C/T$  shown in Fig. 5 for the  $x=0.6$  and  $0.65$  samples. In order to check the field dependence of our specific heat data to compare with that found for  $\chi$  in Ref. 13, field  $C/T$  data were taken and are shown in Fig. 6. Fermi liquid, nondivergent behavior in  $C/T$  is recovered by 8 T; a low field such as 100 G (0.01 T) has a negligible effect on the divergence of the data at low temperatures—contrasting with the  $\chi$  data.<sup>13</sup>

$x=0.65$ : Data for  $x=0.65$  shown in Fig. 5, measured down to 0.3 K, are similar to the  $x=0.6$  data in magnitude and follow  $C/T \sim \log T$  over the entire temperature range of measurement as well. Since the  $\rho_0$  values for the  $x=0.6$  and  $0.65$  samples (see Table I) differ by over 60%, it is clear that the bulk specific heat properties are not strongly dependent on the resistivity behavior. The values for  $T_{\log}$  for  $x=0.6$  and  $0.65, 0.07$ , and  $0.3$  K, respectively, are also shown in Fig. 2 and, just as for  $x=0.4$ , the minimum in  $T_{\log}$  again corresponds with a peak in  $\rho_0$ .

Thus, as  $x$  increases past  $0.5$  in  $\text{Ce}(\text{Ru}_{1-x}\text{Rh}_x)_2\text{Si}_2$ , the specific heat for polycrystalline material switches quickly from saturation behavior in  $C/T$ , consistent with Moriya weak spin fluctuations, to an enormous temperature range of  $C/T \sim \log T$ , indicative<sup>27</sup> of strongly coupled fluctuations. As we have discussed, one way to quantify this temperature

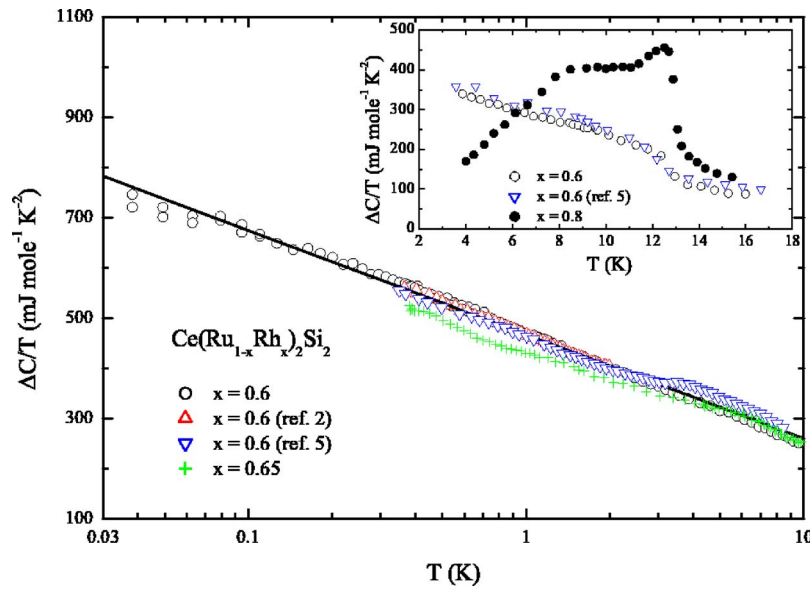


FIG. 5. (Color online) Electronic specific heat of polycrystalline  $\text{Ce}(\text{Ru}_{1-x}\text{Rh}_x)_2\text{Si}_2$ ,  $x=0.6, 0.65$ , and  $0.8$ . Note that  $C/T \sim \log T$  over  $2\ 1/2$  decades in temperature for polycrystalline  $x=0.6$ , with some slight saturation behavior below  $0.08$  K. For the present work, specific heat data measured to  $0.04$  K were measured at Universitaet Augsburg while data to  $0.1$  K were measured in SCM-1 at NHMFL Tallahassee and data down to  $0.3$  K were measured in-house in yet a third calorimeter at the University of Florida. Also, in the inset, note the large anomaly ( $\sim 0.5R \ln 2$  of entropy) at  $T_N=13$  K for  $x=0.8$  vs the rather negligible anomaly ( $\sim 0.03R \ln 2$  of entropy) for polycrystalline  $x=0.6$ . Polycrystalline  $x=0.65$  (not shown) shows approximately the same size anomaly as for the polycrystalline  $x=0.6$ . Since  $\rho_0$  for  $x=0.6$  and  $0.65$  differs by  $60\%$ , this same amount of entropy for the two polycrystalline samples (indicative of the same amount of phase separation) in the two samples is further indication that  $\rho_0$  vs  $x$  is not dominated by the phase separation. Data for  $x=0.7$  (not shown) show an anomaly at  $13$  K approximately  $1/2$  the size of that observed for  $x=0.8$ . Below the anomaly for  $x=0.7$ , the  $\Delta C/T$  data are almost constant (Fermi liquidlike) down to  $1.5$  K, below which there is a small ( $\sim 10\%$ ) upturn down to  $0.3$  K. It is interesting to note that the higher temperature data in the inset from Ref. 5 for their polycrystalline  $x=0.6$  sample show the same size anomaly as found in the present work.

range of  $\log T$  behavior is with the parameter  $T_{\log}$ , as plotted in Fig. 2. This rapid change in  $T_{\log}$  with  $x$  is in contrast to the gradual change seen in the temperature dependence of  $\rho$ , i.e., in the exponent  $\alpha$ , but matches fairly well the sharp two peak structure in  $\rho_0$  at  $x=0.4$  and  $0.65$ .

$x=0.55$ : In order to stress how rapid and complete this change in the temperature dependence of  $C/T$  is, data were

taken for  $x=0.55$  and are presented together with the data for  $x=0.5$  and  $0.6$  in Fig. 7. Clearly, as  $x \rightarrow 0.6$  from the region  $0.4 \leq x \leq 0.5$ , there is still saturation behavior in  $C/T$  for  $x=0.55$  at low temperatures, but the temperature range where  $C/T \sim \log T$  is extended ( $C/T$  is fit by  $\log T$  approximately from  $0.6$  to  $6$  K) for  $x=0.55$  vs the  $x=0.5$  data where  $C/T$  vs  $\log T$  shows much more curvature already as high as  $3-4$  K.

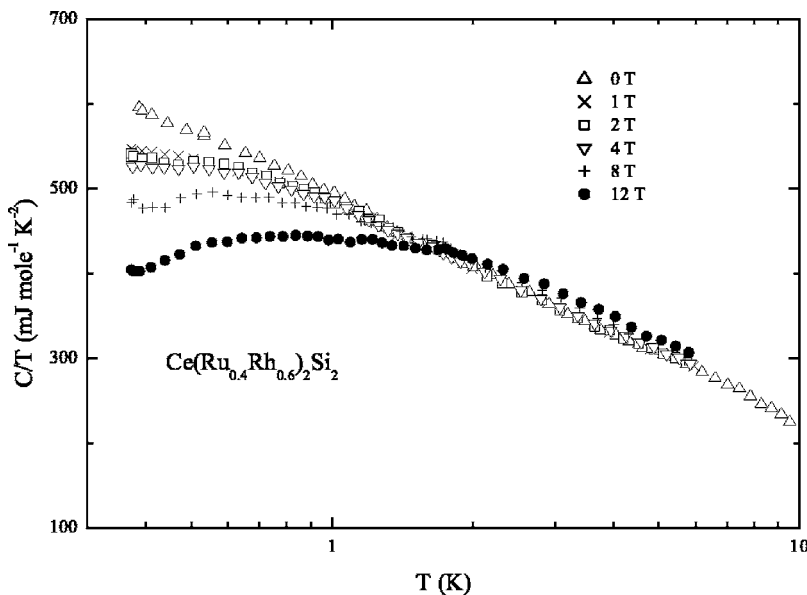


FIG. 6. Specific heat divided by temperature,  $C/T$  (not corrected for the lattice contribution which is independent of magnetic field) vs  $\log T$  for polycrystalline  $\text{Ce}(\text{Ru}_{0.4}\text{Rh}_{0.6})_2\text{Si}_2$  in fields between  $0$  and  $12$  T. Note the return to  $C/T \sim \text{const}$  (Fermi liquid behavior) by  $8$  T.

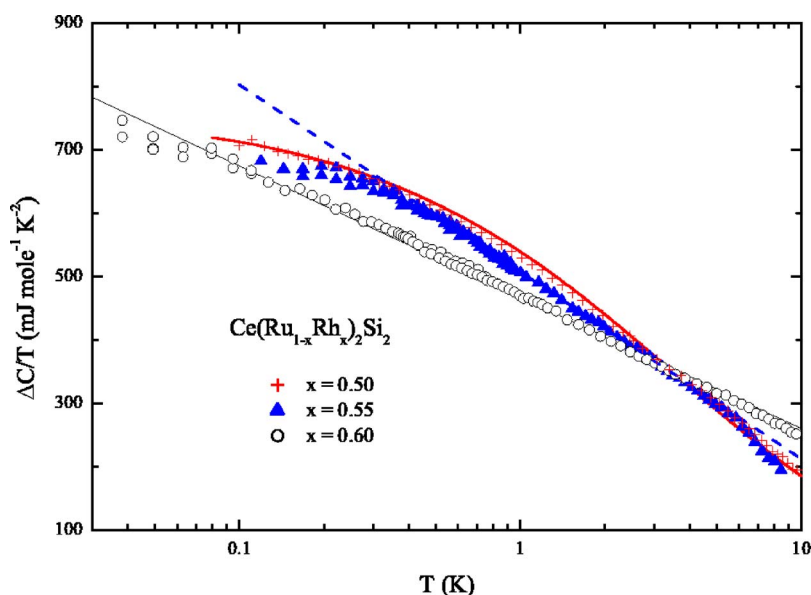


FIG. 7. (Color online) Electronic specific heat of polycrystalline  $\text{Ce}(\text{Ru}_{1-x}\text{Rh}_x)_2\text{Si}_2$ ,  $x=0.5, 0.55$ , and  $0.6$ , allowing a comparison in order to highlight the rapid change in temperature dependence of  $C/T$  with composition. The dashed line (---) through the  $x=0.55$  data shows that  $C/T \sim \log T$  for this composition over a more limited temperature range than for  $x=0.6$ , but over a larger temperature range than for the  $x=0.5$  data. The solid line (—) through the  $x=0.5$  data<sup>6</sup> is the fit to the Moriya theory (Ref. 37) shown in Fig. 4.

#### IV. CONCLUSIONS

The present work provides an overview of the non-Fermi liquid behavior associated with *two* QCP's in the  $\text{Ce}(\text{Ru}_{1-x}\text{Rh}_x)_2\text{Si}_2$  system via measurement of  $\rho$ ,  $\chi$ , and  $C/T$  data for  $x=0.04, 0.3, 0.4, 0.45, 0.5, 0.55, 0.6, 0.65, 0.7$ , and  $0.8$ . Previous results, as well as those of the present work, indicate that the spin density wave magnetic ordering temperature goes to zero around  $x=0.4$ . For polycrystalline  $\text{Ce}(\text{Ru}_{1-x}\text{Rh}_x)_2\text{Si}_2$ ,  $0.4 \leq x \leq 0.5$ ,  $C/T$  data from the present work down to  $0.1$  K show definite non- $\log T$  behavior below a certain temperature defined here as  $T_{\text{log}}$ . This behavior is characteristic of saturation in  $C/T$  and can be fit by the Moriya theory<sup>37</sup> of weak coupled spin fluctuations, but also by other models—not including the Griffiths phase scenario—such as the Kondo disorder model. Data for  $x=0.55, 0.6$ , and  $0.65$ , indicate  $C/T \sim \log T$  down to  $0.6$  (not the lowest temperature of measurement),  $0.04$ , and  $0.3$  K, respectively. This indicates a distinct change in the nature of

the spin fluctuations with doping between  $T_{\text{SDW}}=0$  at  $x \sim 0.4$  and the suppression to  $T=0$  of the local moment antiferromagnetism present in  $\text{Ce}(\text{Ru}_{1-x}\text{Rh}_x)_2\text{Si}_2$  for  $x \leq 0.65$ . These specific heat results, together with the observed sharply defined twin peaks in  $\rho_0$  vs  $x$  at  $x=0.4$  and  $0.65$ , are consistent with two quantum critical points in  $\text{Ce}(\text{Ru}_{1-x}\text{Rh}_x)_2\text{Si}_2$ , as have been proposed by others.<sup>13</sup> The Rh-rich quantum critical point is dominated by strong spin fluctuations which result in  $C/T \sim \log T$  and the Ru-rich side's quantum critical point is dominated by weak spin fluctuations with saturation in  $C/T$  at low temperatures.

#### ACKNOWLEDGMENTS

The work at the University of Florida was carried out under the auspices of the U.S. D.O.E., Contract No. DE-FG02-86ER45268 (J.S.K., D.J.M., D.B., and G.R.S.), NSF Grant No. DMR-0312939 (K.I.), and U.S. D.O.E. Contract No. DE-FG02-99ER45748 (B.A.).

<sup>1</sup>T. Taniguchi, Y. Tabata, and Y. Miyako, J. Phys. Soc. Jpn. **68**, 2026 (1999).

<sup>2</sup>B. Lloret, B. Chevalier, B. Buffat, J. Etourneau, S. Quezel, A. Lamharrar, J. Rossat-Mignod, R. Calemczuk, and E. Bonjour, J. Magn. Magn. Mater. **63**, 85 (1987).

<sup>3</sup>T. Taniguchi, Y. Tabata, H. Tanabe, and Y. Miyako, J. Magn. Magn. Mater. **177**, 419 (1998).

<sup>4</sup>T. Nakano, K. Fujita, Y. Ohmori, S. Murayama, K. Hoshi, H. Amitsuka, Y. Onuki, M. Ocio, and J. Hammann, Physica B **312**, 440 (2002).

<sup>5</sup>R. Calemczuk, E. Bonjour, J. Rossat-Mignod, and B. Chevalier, J. Magn. Magn. Mater. **90**, 477 (1990).

<sup>6</sup>T. Graf, J. D. Thompson, M. F. Hundley, R. Movshovich, Z. Fisk, D. Mandrus, R. A. Fisher, and N. E. Phillips, Phys. Rev. Lett. **78**, 3769 (1997).

<sup>7</sup>T. Nakano, Y. Ohmori, S. Murayama, K. Hoshi, and Y. Onuki, Physica B **281**, 346 (2000).

<sup>8</sup>S. Kawarazaki, Y. Kobashi, J. A. Fernandez-Baca, S. Murayama, Y. Onuki, and Y. Miyako, Physica B **206**, 298 (1995).

<sup>9</sup>S. Kawarazaki, M. Sata, H. Kadowaki, Y. Yamamoto, and Y. Miyako, J. Phys. Soc. Jpn. **66**, 2473 (1997).

<sup>10</sup>Y. Tabata, T. Taniguchi, and Y. Miyako, Physica B **312**, 433 (2002).

<sup>11</sup>Y. Tabata, T. Taniguchi, Y. Yamamoto, Y. Miyako, M. Ocio, P. Pari, and J. Hammann, Physica B **281**, 349 (2000).

<sup>12</sup>Y. Tabata, T. Taniguchi, K. Yamanaka, and S. Kawarazaki, J. Magn. Magn. Mater. **272**, 197 (2004).

<sup>13</sup>Y. Tabata, T. Taniguchi, Y. Miyako, O. Tegus, A. A. Menovsky, and J. A. Mydosh, Phys. Rev. B **70**, 144415 (2004).



- <sup>14</sup>C. Sekine, T. Sakakibara, H. Amitsuka, Y. Miyako, and T. Goto, *J. Phys. Soc. Jpn.* **61**, 4536 (1992).
- <sup>15</sup>H. W. Gu, J. Tang, A. Matsushita, T. Taniguchi, Y. Tabata, and Y. Miyako, *Physica B* **312**, 248 (2002).
- <sup>16</sup>D. E. MacLaughlin, O. O. Bernal, J. E. Sonier, R. H. Heffner, T. Taniguchi, and Y. Miyako, *Phys. Rev. B* **65**, 184401 (2002).
- <sup>17</sup>C. H. Booth, S.-W. Han, S. Skanthakumar, and J. L. Sarrao, *Physica B* **354**, 313 (2004).
- <sup>18</sup>J. Souletie, Y. Tabata, T. Taniguchi, and Y. Miyako, *Physica B* **259**, 372 (1999).
- <sup>19</sup>H. Kadowaki, Y. Tabata, M. Sato, N. Aso, S. Raymond, and S. Kawarazaki, *Phys. Rev. Lett.* **96**, 016401 (2006).
- <sup>20</sup>Y. Tabata, D. R. Grempel, M. Ocio, T. Taniguchi, and Y. Miyako, *Phys. Rev. Lett.* **86**, 524 (2001).
- <sup>21</sup>C. L. Seaman, M. B. Maple, B. W. Lee, S. Ghamaty, M. S. Torikachvili, J.-S. Kang, L. Z. Liu, J. W. Allen, and D. L. Cox, *Phys. Rev. Lett.* **67**, 2882 (1991).
- <sup>22</sup>J. D. Thompson, J. O. Willis, C. Godart, D. E. MacLaughlin, and L. C. Gupta, *J. Magn. Magn. Mater.* **47**, 281 (1985).
- <sup>23</sup>For a review of CeRu<sub>2</sub>Si<sub>2</sub> properties, see J. Flouquet, S. Kambe, L. P. Regnault, P. Haen, J. P. Brison, F. Lapierre, and P. Lejay, *Physica B* **215**, 77 (1995).
- <sup>24</sup>K. Heuser, E.-W. Scheidt, T. Schreiner, Z. Fisk, and G. R. Stewart, *J. Low Temp. Phys.* **118**, 235 (2000).
- <sup>25</sup>B. H. Grier, J. M. Lawrence, V. Murgai, and R. D. Parks, *Phys. Rev. B* **29**, 2664 (1984).
- <sup>26</sup>R. Movshovich, T. Graf, D. Mandrus, J. D. Thompson, J. L. Smith, and Z. Fisk, *Phys. Rev. B* **53**, 8241 (1996).
- <sup>27</sup>For a review, see G. R. Stewart, *Rev. Mod. Phys.* **73**, 797 (2001). See also G. R. Stewart, *ibid.* **78**, 743 (2006).
- <sup>28</sup>G. R. Stewart, *Rev. Sci. Instrum.* **54**, 1 (1983); H. Tsujii, B. Andraka, E. C. Palm, T. P. Murphy, and Y. Takano, *Physica B* **329**, 1638 (2003).
- <sup>29</sup>For a more thorough discussion of the phase separation, see J. S. Kim, D. J. Mixson, D. Burnette, and G. R. Stewart (unpublished).
- <sup>30</sup>A. deVisser, A. Menovsky, and J. J. M. Franse, *Physica B & C* **147**, 81 (1987).
- <sup>31</sup>S. A. Grigera, R. S. Perry, A. J. Schofield, M. Chiao, S. R. Julian, G. G. Lonzarich, S. I. Ikeda, Y. Maeno, A. J. Millis, and A. P. MacKenzie, *Science* **294**, 329 (2001).
- <sup>32</sup>M. H. Jung and Y. S. Kwon, *Physica B* **359**, 59 (2005).
- <sup>33</sup>M. S. Wire, Ph.D thesis, Univ. of California at San Diego, Los Alamos National Laboratory Report No. LA-10199-T, available from National Technical Information Service, US Dept. of Commerce, document number DE85005317. See also M. S. Wire *et al.*, *Phys. Rev. B* **27**, 6518 (1983).
- <sup>34</sup>F. Lapierre, P. Haen, T. Jaworska, and P. Lejay, *Physica B* **284**, 1259 (2000).
- <sup>35</sup>J. S. Kim, B. Andraka, G. Fraunberger, and G. R. Stewart, *Phys. Rev. B* **41**, 541 (1990).
- <sup>36</sup>Y. Tabata, T. Taniguchi, M. Sato, S. Kawarazaki, and Y. Miyako, *J. Phys. Soc. Jpn.* **67**, 2484 (1998).
- <sup>37</sup>T. Moriya and T. Takimoto, *J. Phys. Soc. Jpn.* **64**, 960 (1995).
- <sup>38</sup>A. H. Castro Neto, G. Castilla, and B. A. Jones, *Phys. Rev. Lett.* **81**, 3531 (1998); A. H. Castro Neto and B. A. Jones, *Phys. Rev. B* **62**, 14975 (2000).
- <sup>39</sup>A study on single crystalline Ce(Ru<sub>1-x</sub>Rh<sub>x</sub>)<sub>2</sub>Si<sub>2</sub>, using a preparation technique pioneered by Fisk and Remeika [unpublished, but see, e.g., J. S. Kim, D. Hall, P. Kumar, and G. R. Stewart, *Phys. Rev. B* **67**, 014404 (2003); and K. Heuser, E.-W. Scheidt, T. Schreiner, Z. Fisk, and G. R. Stewart, *J. Low Temp. Phys.* **118**, 235 (2000)] is planned.